This article has been accepted for publication in a future issue of this journal, but has not been fully edited. Content may change prior to final publication. Citation information: DOI 10.1109/JSEN.2019.2907143, IEEE Sensors Journal

Digital Matched Filtering (DMF) Technique for The Performance Enhancement of Few-mode Fibre Bragg Grating Sensor

Muhammad Khairol Annuar Zaini, Yen Sian Lee, Kok-Sing Lim, Muhammad Mahmood Ali, Nurul Asha Mohd Nazal, and Harith Ahmad

***Abstract*—In this work, the digital matched filtering (DMF), a signal processing technique, has been proposed to identify the multiple peak wavelengths, more accurately from reflection spectra of etched few-mode fibre Bragg grating (FM-FBG) sensor. The etched FM-FBG has been fabricated and its intrinsic property of having different sensitivities for different reflection peaks in spectrum has been used for sensing the multiple parameters, such as temperature and refractive index of the ambient environment. The experimental characterization of the fabricated etched FM-FBG sensor has been carried out by using six samples of standard sodium chloride ($NaCl_{(aq)}$) solutions with refractive indices (RIs) ranging from 1.3159 to 1.3375 at 24 °C temperature. The reflection spectra have been acquired for each sample by varying the temperature from 24 °C to 80 °C. The temperature and RI sensitivities have been investigated from the acquired spectra by using digital matched filter (DMF). The obtained sensor results have been compared with conventional peak detection (CPD) method results for the same spectra. It has been observed that the results obtained by DMF technique are closer to the reference sensor values and has shown more accuracy than the results obtained by CPD technique. It has been shown that the DMF has better performance in terms of the accuracy of measured results than that of CPD. In addition, to eliminate the effect of cross sensitivity issue of the sensor, the 3×3 order characteristic matrix has been used. Hence, the etched FM-FBG can be used as multi-parameter measurements with better performance using DMF technique.**

***Index Terms*—Fibre Bragg gratings (FBGs), optical fibre sensors, Digital matched filtering signal processing technique.**

I. Introduction

FIBRE Bragg grating (FBG) based sensors have been playing a vital role in sensing technology due to their compact size, multiplexing capability, high sensitivity, and suitability for remote sensing [1], [2]. Single-mode fibre (SMF) has been commonly used in the study of FBG sensors due to its compatibility with the existing technologies such as optical communication. However, due to its single peak wavelength in reflection spectrum, one can only measure single physical parameter at a time. So far, many researchers have worked on single mode FBG for various applications by enhancing its performance in terms of sensitivity, accuracy and stability. In addition to many single parameter sensing with single mode FBG, the simultaneous measurements by single probe sensor utilising the hybrid structure of FBG and different interferometers or long period grating (LPG), have also been reported [3-5]. But, these hybrid sensors for multi-parameter sensing have some structural and fabrication complexities. On the other hand, recently, with the introduction of space division multiplexing (SDM) technology, the few mode fiber (FMF) has become the strong candidate for future communication technologies due to its capability to accommodate larger number of spatial modes (2-mode, 4-mode fibers and etc.). Therefore, the FBG fabrication in FMF has been introduced which gives the multiple peak wavelengths in the reflection spectrum corresponding to their mode numbers. These peaks at different wavelengths correspond to the self- or cross-coupling of the guided modes in the FMF. Perturbation in the period of the few-mode FBG (FM-FBG) or the effective refractive index (ERID) of the guided modes will lead to the shift in the resonant wavelength. Calibration can be made to determine the relationships between the wavelength shift and the changes in the corresponding measurands. Several theoretical and experimental studies have been performed on the applications and the characteristics of FM-FBG [6-11]. Moreover, it has been reported that each mode in few-mode fibre Bragg grating (FM-FBG) shows different sensitivity towards the physical parameter and therefore it can be used as multi-parameter sensor [12-15]. Nevertheless, the development of a multi-parameter sensor based on only a single sensing element like FM-FBG, is hindered by a major limitation which is cross-sensitivity problem inherited from the sensor property [16-17]. Fortunately, this can be resolved by using 3x3 order characteristic matrix for discriminative measurement reported by Yang *et al.* [15]. Yang *et al.* demonstrated a cladless FM-FBG based sensor for simultaneous temperature and RI measurement in which with the assistance of 3×3 characteristic matrix, discrimination measurements of temperature and RI has been demonstrated.

This work was supported by the FRGS (FP033-2017A).

M.K.A. Zaini, Y.S. Lee, K.S. Lim, N.A.M. Nazal and H. Ahmad are with the Photonics Research Centre, University of Malaya, Kuala Lumpur, 50603, Malaysia. (emails: annuarzaini4565@gmail.com; yensian1110@gmail.com; kslim@um.edu.my). H. Ahmad is with the Photonics Research Centre, University of Malaya, Kuala Lumpur, 50603, Malaysia and also with the Department of Physics, Faculty of Science and Technology, Airlangga University, Surabaya 60115, Indonesia. (email: harith@um.edu.my). M. M. Ali is with Optical Fiber Sensor Research Centre, Department of Electronic and Computer Engineering, University of Limerick, Limerick, V94 T9PX, Ireland. (email: engrmahmoodnaz@gmail.com).

1558-1748 (c) 2018 IEEE. Personal use is permitted, but republication/redistribution requires IEEE permission. See http://www.ieee.org/publications_standards/publications/rights/index.html for more information.

This article has been accepted for publication in a future issue of this journal, but has not been fully edited. Content may change prior to final publication. Citation information: DOI 10.1109/JSEN.2019.2907143, IEEE Sensors Journal

Chemical etching technique was used for reducing the fibre diameter or removal of the fibre cladding which enhanced the evanescent fields of the core modes and sensitive to change in the ambient medium. In the context of grating imprinted in an etched FMF, the changes in the surrounding refractive index (SRI) influence the effective refractive index (ERI) of various modes propagating across the grating and consequently, influencing the corresponding resonant wavelengths of the grating. Due to the extended mode fields of HOMs, the associated resonant wavelengths are generally more sensitive to the change in SRI. The higher is the mode order, the greater is the sensitivity. While the use of HOM can enhance the detection sensitivity of FBG sensor towards RI change, improvement in the capability to detect small resonant wavelength shift can increase the measurement accuracy [13]. In addition, several schemes have been reported for detecting the wavelength shift in FBG sensors by using either a broadband source or various spectral analysis techniques such as edge filters, scanning Fabry-Perot filters, acousto-optic tuneable filters, Mach-Zehnder interferometers, or a tuneable laser source with a broadband detector and Nevertheless, for each of the schemes, the wavelength detection accuracy is limited by various types of noise. Sensing systems employing broadband sources generally have low signal-to-noise ratio (SNR) due to the low output signal power. On the other hand, systems employing laser sources have higher SNR but residual reflections in the systems often lead to undesired interferometric signals that would limit the accuracy of wavelength measurement.

Numerous signal processing techniques for enhancing the detection accuracy have been reported to enhance the SNR and also measurement accuracy [18-20]. One of the common techniques, is to use a tuneable filter to scan through the reflected spectrum of the grating and then measure the filtered wavelength corresponding to the maximum of the system's output. This is known as conventional peak detection (CPD) technique and it can be easily applied to interrogate a number of FBG sensors based on WDM principle [19-20]. However, the accuracy of the CPD technique is limited when the level of the reflected signal is low. Meanwhile, techniques based on signal processing methods such as minimum variance shift (MVS) [21] and spectrum correlation (SC) [22], have also been proposed.

Multi-wavelength detection gives an extra advantage for detection sensitivity, because each of the resonant peaks has their own sensitivity. Therefore, the detection of each peak is significant because the signal-to-noise ratio (SNR) of higher order modes is at lower level than fundamental mode. However, sometimes the FBG spectrum presents undesirable side lobes on the fundamental peak due to Fabry-Perot resonances at the boundaries of the FBG that can interferes the neighbouring peaks. The suppression of the side lobes in the reflection spectrum can enhance the detection and measurement accuracy of the FM-FBG sensor. Therefore, a digital matched filtering (DMF) technique has been proposed to reduce the effect of side lobes in the spectrum of etched FM-FBG which consequently, leads to a better accuracy in sensing measurement [23].

In this paper, we demonstrate that digital matched filtering (DMF) technique can enhance the detection accuracy of resonant wavelength shift in an etched FM-FBG. In section 2, the theoretical background of both the CPD and DMF techniques, will be presented. In section 3, the experimental setup and methodology for acquiring the measurement results will be demonstrated. Whereas, in section 4, the acquired results and the accuracy of the proposed DMF technique are discussed. It can be seen in the results that DMF technique has enhanced the performance of the multi-parameter sensor and hence can be used in many applications of FM-FBG based sensors. Finally, the conclusion is drawn in section 5.

II. THEORETICAL BACKGROUND OF CPD AND DMF TECHNIQUES

In the CPD technique, peak wavelength is determined by taking the wavelength corresponding to the local maximum value of the spectrum. However, when the SNR is low, high frequency component in the signal may lead to inaccuracy in the determination of peak wavelength. In contrast, the DMF technique determines the peak wavelength by matching the peaks in a signal with a Gaussian peak. The frequency response of the DMF is matched to the signal frequency and the noise in the signal will be filtered since it is not matched with the signal frequency. This allows the DMF technique to provide measurement of wavelength shift with better accuracy in the case of low SNR.

A filter that matched to a physical waveform, *s(t)* is one with impulse response [23, 24]:

$$h(\tau) = \mathrm{k}\, s(\Delta - \tau) \tag{1}$$

where k and Δ are arbitrary constant. The Fourier transform of the impulse response which is the transfer function for DMF will have the following form:

$$\begin{aligned} H(j\omega) &= \int_{-\infty}^{\infty} h(\tau)\, e^{-j\omega\tau}\, d\tau \\ &= \mathrm{k} \int_{-\infty}^{\infty} s(\Delta - \tau)\, e^{-j\omega\tau}\, d\tau \\ &= \mathrm{k}\, e^{-j\omega\Delta} \int_{-\infty}^{\infty} s(\tau')\, e^{-j\omega\tau'}\, d\tau' \end{aligned} \tag{2}$$

where $\tau' = \Delta - \tau$, $\omega = 2\pi f$ in radians with f as the operating frequency in Hz. Meanwhile, the Fourier transform of *s(t)* is:

$$S(j\omega) = \int_{-\infty}^{\infty} s(t)\, e^{-j\omega\tau}\, dt. \tag{3}$$

Comparing (2) and (3) gives:

$$\begin{aligned} H(j\omega) &= \mathrm{k}\, S(-j\omega)\, e^{-j\omega\Delta} \\ &= \mathrm{k}\, S^*(j\omega)\, e^{-j\omega\Delta} \end{aligned} \tag{4}$$

where S^* is the complex conjugate of S. Therefore, the transfer function for DMF is equivalent to the complex conjugate of the Fourier transform of s(t) except $\mathrm{k}e^{-j\omega\Delta}$ with possible amplitude and delay factor.

III. EXPERIMENTAL SETUP AND METHODOLOGY

FM-FBG being used in this work was fabricated by inscribing uniform FBG in the core of four-mode step index fibre (4MF; OFS, Denmark) using the phase mask technique. The 4MF has core diameter of 19.5 um while the RIs of the core and cladding are 1.444 and 1.449 respectively. Prior to the FBG inscription, the 4MF was kept in a high pressure

1558-1748 (c) 2018 IEEE. Personal use is permitted, but republication/redistribution requires IEEE permission. See http://www.ieee.org/publications_standards/publications/rights/index.html for more information.

This article has been accepted for publication in a future issue of this journal, but has not been fully edited. Content may change prior to final publication. Citation information: DOI 10.1109/JSEN.2019.2907143, IEEE Sensors Journal

(2000 psi) hydrogen tank for 1 week to enhance the photosensitivity of the fibre. Krypton fluoride (KrF) excimer laser with peak wavelength of 248 nm and phase mask with a period of 1068.80 nm was used. The FBG inscribed in the 4MF core has a length of 2 cm. After the inscription process, the FM-FBG was annealed in oven at 70 °C for 8 hours to out-diffuse the residual hydrogen in the fibre.

After the fabrication of an FM-FBG, the cladding was chemically etched by Buffered Oxide Etchant (BOE) solution with HF:NH_4OH composition of 1:6. The etchant was covered with a layer of silicon oil to prevent the evaporation of the solution. The FM-FBG was connected to an erbium-doped fibre amplifier (EDFA) and the reflection spectrum of the FM-FBG was continuously monitored by an optical spectrum analyser (OSA, ANDO AQ-6331) during the etching process. The OSA was controlled by LabVIEW program in a computer via GPIB interface to save the measured spectrum into the computer at an interval of 2 minutes. The etching process was stopped when the Bragg wavelength in the reflection spectrum shifted about 3 nm from its initial value. Next, the FM-FBG was removed from the etchant and rinsed with distilled water to remove the residual etchant on the surface of the etched FM-FBG. After that, the final diameter of the FM-FBG was measured by an optical microscope as shown in figure 1. Following that, the mode corresponding to each resonant wavelength was estimated theoretically and it will be discussed in detail in section 4. The response of the resonant wavelengths towards the change in RI and temperature was examined by dipping the FM-FBG into sodium chloride ($NaCl_{(aq)}$) solutions with different concentrations and temperatures. The complete experimental setup used for sensor data acquisition has been shown in figure 2. Six samples of standard $NaCl_{(aq)}$ solutions were prepared with refractive indices (RIs) ranging from 1.3159 to 1.3375 at 24 °C temperature. For characterization of the sensor, the range of temperature was considered as 24 °C – 80 °C respectively. A hot plate with temperature resolution of 0.1 °C was used to heat the solution at different temperatures. The aforementioned reference RIs of the solutions were measured by a prism coupler at the wavelength of 1550 nm to evaluate the accuracy of the RI values determined by the etched FM-FBG sensor. Meanwhile, the reference temperature was measured through thermocouple positioned near to the sensor in the solution during the measurement. Before dipping the sensor into the solution, a reference reflection spectrum corresponding to the RI of air and room temperature was recorded.

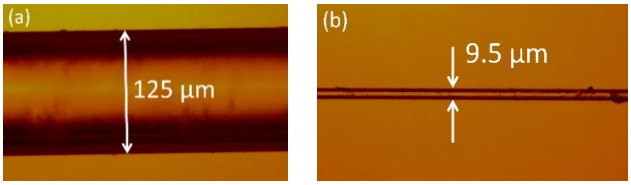

Fig. 1. *Micrographs of the few mode fibre: (a) before etching (b) after etching*.

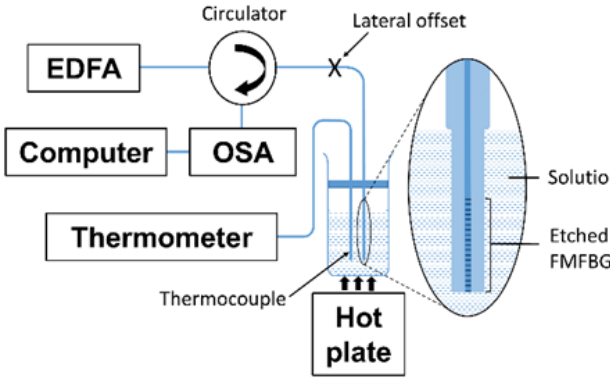

Fig. 2. *Experimental setup used for sensor data acquisition. EDFA: Erbium doped fibre amplifier, OSA: Optical spectrum*

When the etched FM-FBG was dipped in the $NaCl_{(aq)}$ solution with a specific RI at room temperatures, the reflection spectrum was recorded by the OSA and saved in the computer. The temperature of the solution was then gradually increased by the hot plate. At different temperatures, the reflection spectrum was saved. Before the spectrum was saved, the hot plate was maintained at the same temperature for 10 minutes to ensure the homogeneous distribution of the temperature in the solution. The procedure was repeated for $NaCl_{(aq)}$ solution with different RIs. Then, the saved raw spectra were processed by CPD technique to determine the shift of the resonant wavelengths corresponding to self- or cross-coupling of the transverse modes. From the wavelength shift, the sensitivity of each resonant wavelength towards RI and temperature change was calculated.

After that, the same set of raw spectra was processed by the DMF technique and determination of the resonant wavelengths' sensitivity towards RI and temperature change was repeated. The results obtained by the CPD and DMF technique were then compared with the reference values to verify the measurement accuracy of each technique.

IV. RESULTS AND DISCUSSION

The reflection spectra of the FM-FBG before and after the etching process is shown in figure 3. It is evident from the spectra of figure 3 that the number of resonant wavelength increased from five to six after the etching process.

The mode coupling corresponding to each resonant wavelength can be estimated by determining the intersection between the function f(λ) and g(λ), where:

$$g(\lambda) = \lambda \tag{5}$$

$$f(\lambda) = \begin{cases} 2n_{eff,\mu}\,\Lambda & ; \text{ self-coupling} \\ \left(n_{eff,\mu} + n_{eff,\nu}\right)\Lambda & ; \text{ cross-coupling} \end{cases} \tag{6}$$

where $n_{eff,\mu/\nu}$ is the effective refractive index of transverse mode $LP_{\mu/\nu}$, $\mu,\ \nu \in \{01, 11, 02\}, \mu \neq \nu$, and Λ is the grating period. Based on the intersections, λ_1, λ_2, λ_3, λ_4, λ_5, and λ_6 correspond to mode couplings of $LP_{01}^{+} \leftrightarrow LP_{01}^{-}$, $LP_{01}^{+} \leftrightarrow LP_{11}^{-}$, $LP_{11}^{+} \leftrightarrow LP_{11}^{-}$, $LP_{01}^{+} \leftrightarrow LP_{21}^{-}$, $LP_{11}^{+} \leftrightarrow LP_{02}^{-}$, and $LP_{21}^{+} \leftrightarrow LP_{21}^{-}$ respectively.

1558-1748 (c) 2018 IEEE. Personal use is permitted, but republication/redistribution requires IEEE permission. See http://www.ieee.org/publications_standards/publications/rights/index.html for more information.

This article has been accepted for publication in a future issue of this journal, but has not been fully edited. Content may change prior to final publication. Citation information: DOI 10.1109/JSEN.2019.2907143, IEEE Sensors Journal

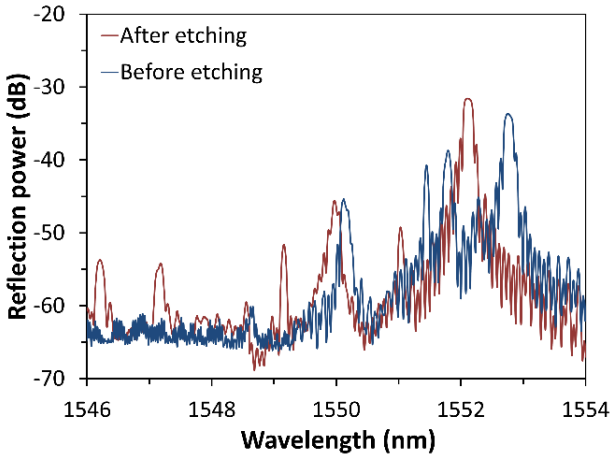

Fig. 3. *Reflection spectra of the FM-FBG acquired before and after the etching process.*

When the etched FM-FBG was dipped in NaCl solution with different temperature or RI, red-shift was observed in the resonant wavelengths of the reflection spectrum. This is shown in Figure 4. In Figure 4(b), the shift in the resonant wavelengths is very small when the SRI increased from 1.3159 to 1.3375. The inset in Figure 4(b) shows the small shift when the SRI is changed. It is observed that the higher-order modes (λ_2, λ_3, λ_4, λ_5, and λ_6) are more sensitive towards the RI and temperature changes as compared to fundamental mode (λ_1) based on the observation on the wavelength shift. The spectra were processed by both CPD and DMF techniques to compare the difference in the values of wavelength shift determined by the different techniques.

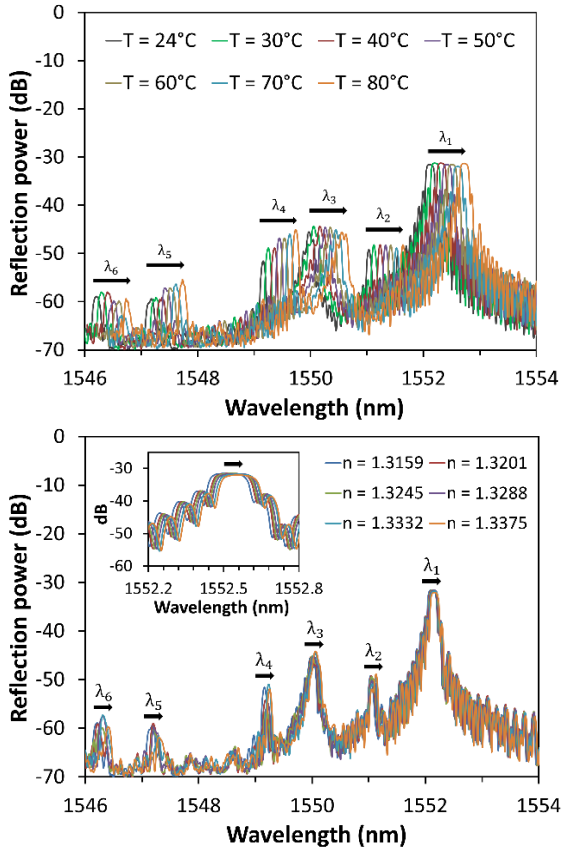

Fig. 4. *Reflection spectra of the etched FM-FBG sensor at different (a) temperature (RI of NaCl solution was fixed at 1.3159) and (b) RI (temperature was fixed at 24 °C).*

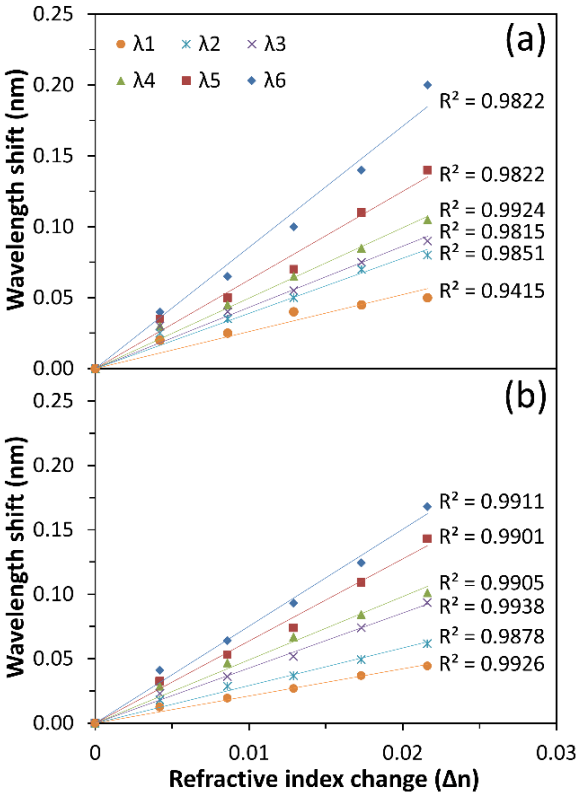

Fig. 5. *Relationship between the refractive index change and the wavelength shift at room temperature (24°C) for different peaks in the etched FM-FBG spectra by using: (a) CPD and (b) DMF.*

The results processed by CPD technique will first be discussed. Figure 5(a) shows the typical relationship between the wavelength shift and the refractive index change for the six peaks, as determined by CPD technique when the temperature is fixed at 24 °C. On the other hand, the relationship between wavelength shift and the temperature change when the RI is varied from 1.3159 to 1.3375 has been determined for peak λ_1 and λ_6. This is shown in Figure 6. Based on the results in Figure 6, the variation of temperature sensitivities with the refractive index change is determined for peak λ_1 and λ_6 and shown in Figure 7. The standard deviation of the temperature sensitivity at different RI change is 0.0001 for the case of λ_1 when the spectra were processed by CPD technique. It is reduced by almost half to 0.00005 when DMF technique was used. On the other hand, the standard deviation is 0.001 for the case of λ_6 when the spectra were processed by CPD technique. When DMF technique was used, the standard deviation reduced to 0.0004.

Since the FM-FBG will react to both temperature and RI, the relationship between the wavelength shift and the temperature and RI change can be determined by solving the following matrix equation:

$$\begin{bmatrix} \Delta n \\ \Delta T \\ \Delta n \Delta T \end{bmatrix} = \begin{bmatrix} K_{n1} & K_{T1} & (K_{Tn1}+K_{nT1}) \\ K_{n2} & K_{T1} & (K_{Tn2}+K_{nT2}) \\ K_{n3} & K_{T1} & (K_{Tn3}+K_{nT3}) \end{bmatrix}^{-1} \begin{bmatrix} \Delta\lambda_1 \\ \Delta\lambda_2 \\ \Delta\lambda_3 \end{bmatrix} \quad (7)$$

1558-1748 (c) 2018 IEEE. Personal use is permitted, but republication/redistribution requires IEEE permission. See http://www.ieee.org/publications_standards/publications/rights/index.html for more information.

This article has been accepted for publication in a future issue of this journal, but has not been fully edited. Content may change prior to final publication. Citation information: DOI 10.1109/JSEN.2019.2907143, IEEE Sensors Journal

where Δn and ΔT are the change in RI and temperature respectively, K_{n1} and K_{T1} are the calibrated sensitivities of RI and temperature respectively while $\Delta\lambda$ is the corresponding wavelength shift. The calibrated sensitivities of RI can be determined from the slope of the linear plot in Figure 5 while that for temperature can be determined from the y-intercept of the linear plot in figure 7.

The absolute temperature and RI can be obtained by the following equations:

$$n = n_0 + \Delta n \quad (8)$$

$$T(°C) = T_0 + \Delta T \quad (9)$$

where T_0= 24°C and n_0= 1.3159. The values of temperature and RI of the NaCl solutions are obtained by determining the wavelength shift in peak λ_1 and λ_6 using the above methodology. After that, they are compared with the reference RI and temperature measured by prism coupler and thermocouple respectively. This is shown in figure 8(a). The above procedures are repeated by processing the reflection spectra using the DMF technique.

It can be observed that the temperature and RI values determined by the wavelength shift obtained using CPD technique do not match well with the reference values as compared to that obtained by the DMF technique. This is because the small shift in the resonant wavelength can be detected when by the DMF technique. Furthermore, DMF is capable to detect weak signals in a noisy environment when the signal-to-noise ratio (SNR) is low. In the observation, DMF technique obtains a better RI sensitivity with good average linearity, $R^2 \approx 99\%$ as shown in Figure 5. The DMF technique is more accurate than CPD technique because DMF has a frequency response exactly matched to the signal and allows the passage of all the signal frequencies [17]. Thus, it is able to detect the small shift in the resonant wavelengths and led to a more accurate RI and temperature measurement. The results are shown in figure 8(b). Measurement error for the temperature by CPD and DMF technique are ~2.66 °C and ~0.86 °C respectively, whereas for the RI determined by CPD and DMF technique are 0.0006 and 0.0003 respectively.

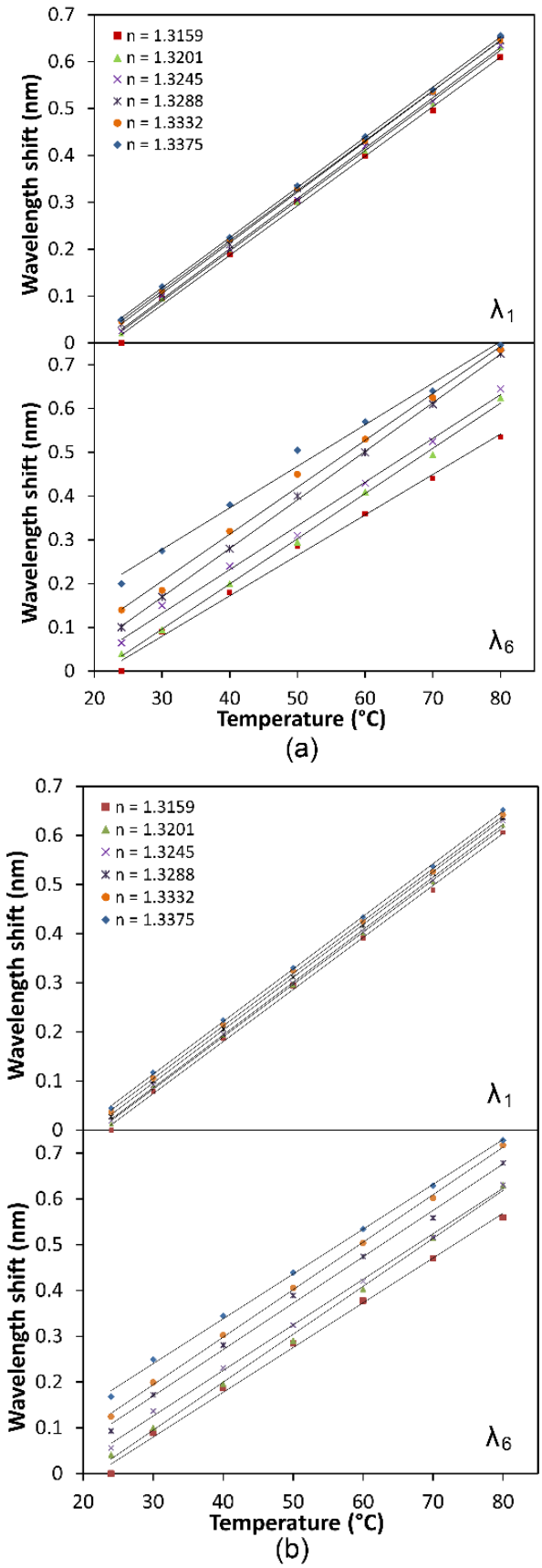

Fig. 6. *Relationship between the wavelength shift and temperature change for solutions with different RIs, as determined from different peaks: (a) CPD and (b) DMF.*

1558-1748 (c) 2018 IEEE. Personal use is permitted, but republication/redistribution requires IEEE permission. See http://www.ieee.org/publications_standards/publications/rights/index.html for more information.

This article has been accepted for publication in a future issue of this journal, but has not been fully edited. Content may change prior to final publication. Citation information: DOI 10.1109/JSEN.2019.2907143, IEEE Sensors Journal

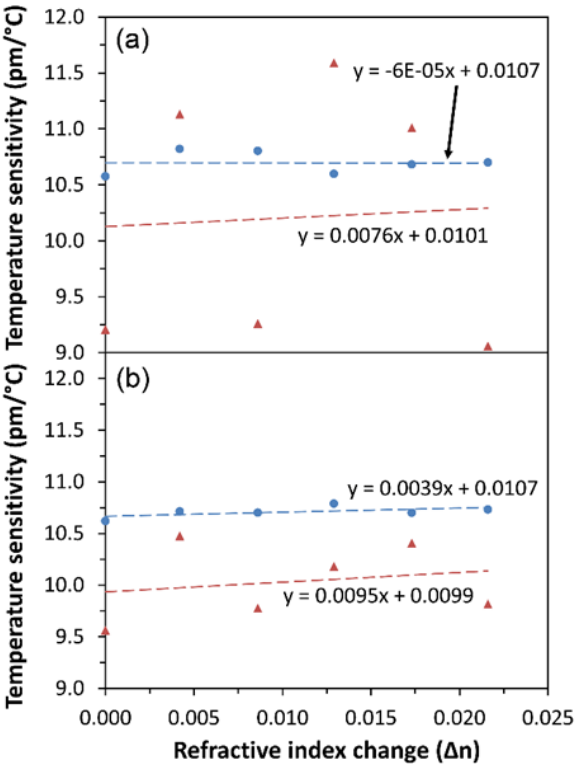

Fig. 7. *Variation of temperature sensitivity at different of solution RI for peak λ_1 and λ_6: (a) CPD technique and (b) DMF.*

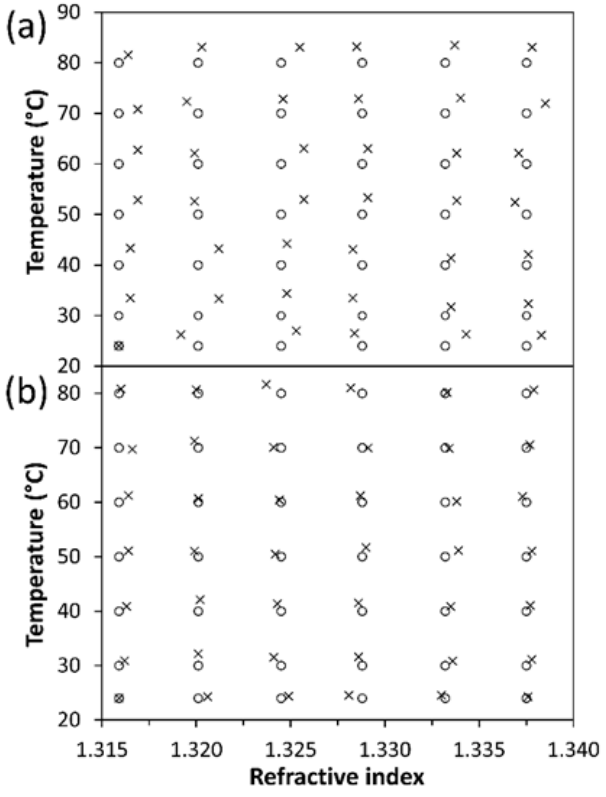

Fig. 8. *Comparison between the measured data sensor and the reference data for (a) CPD and (b) DMF techniques.*

V. Conclusion

In this work, signal processing technique, digital matched filtering, has been utilized to identify the multiple reflection wavelength peaks of etched few-mode fibre Bragg grating (FM-FBG) sensor. To verify the suitability of the proposed method the results were also acquired by CPD technique. The experimental characterization of fabricated sensor was done for six samples of standard $NaCl_{(aq)}$ solutions with initial refractive indices (RIs) at 24 °C ranges from 1.3159 to 1.3375 and at different temperature ranges from 24 °C to 80 °C. For all the acquired spectra, standard deviations for the temperature determined by CPD and DMF techniques are 2.66 °C and 0.86 °C, respectively whereas for the RI the standard deviations determined by CPD and DMF techniques are 0.0006 and 0.0003, respectively. The characterized model of linear system of equations has also been presented with the characteristic matrix of order 3×3 and also the effect of cross sensitivity issue was resolved. It is obvious that the DMF has better performance in terms of the accuracy of measured results with respect to the reference data than that of CPD. The proposed sensing device has potential applications in chemical and biomedical industries for in situ monitoring of temperature and refractive index of the ambient solution.

References

1. E. Udd, W. B. Spillman, *Fiber Optic Sensors: An Introduction for Engineers and Scientists*, 2nd ed.; Wiley: Hoboken, NJ, USA, 2011.
2. R. Kashyap, *Fiber Bragg Gratings*, 2nd ed., Academic Press, USA, 2010.
3. C. Jesus, P. Caldas, O. Frazão, J. L. Santos, P. A. S. Jorge, and J. M. Baptista, "Simultaneous Measurement of Refractive Index and Temperature Using a Hybrid Fiber Bragg Grating/Long-Period Fiber Grating Configuration," Fiber and Integrated Optics, vol. 28, no. 6, pp. 440–449, 2009.
4. S. Gao, W. Zhang, H. Zhang, P. Geng, W. Lin, B. Liu, Z. Bai, and X. Xue, "Fiber modal interferometer with embedded fiber Bragg grating for simultaneous measurements of refractive index and temperature," Sensors and Actuators B: Chemical, vol. 188, pp. 931–936, 2013.
5. Q. Yao, H. Meng, W. Wang, H. Xue, R. Xiong, B. Huang, C. Tan, and X. Huang, "Simultaneous measurement of refractive index and temperature based on a core-offset Mach–Zehnder interferometer combined with a fiber Bragg grating," Sensors and Actuators A: Physical, vol. 209, pp. 73–77, 2014.
6. W. Morey, S. Hewlett, J. Love, and G. Meltz, "Mode-coupling characteristics of UV-written Bragg gratings in depressed-cladding fibre," Electronics Letters, vol. 30, no. 9, pp. 730–732, 1994.
7. T. Mizunami, "Multimode fiber Bragg gratings - spectral characteristics and applications," 11th International Conference on Integrated Optics and Optical Fibre Communications. 23rd European Conference on Optical Communications IOOC-ECOC97, 1997.
8. T. Mizunami, T. Djambova, T. Niiho, and S. Gupta, "Bragg gratings in multimode and few-mode optical fibers," Journal of Lightwave Technology, vol. 18, no. 2, pp. 230–235, 2000.
9. K. H. Wanser, K. F. Voss, and A. D. Kersey, "Novel fiber devices and sensors based on multimode fiber Bragg gratings," Tenth International Conference on Optical Fibre Sensors, 1994.
10. T. Mizunami, T. Niiho, and T. V. Djambova, "Multimode fiber Bragg gratings for fiber optic bending sensors," Proc. SPIE., vol. 3746, pp. 216–219, 1999.
11. B. Sun, A. Wang, L. Xu, C. Gu, Y. Zhou, Z. Lin, H. Ming, and Q. Zhan, "Transverse mode switchable fiber laser through wavelength tuning," Optics Letters, vol. 38, no. 5, p. 667, 2013.

1558-1748 (c) 2018 IEEE. Personal use is permitted, but republication/redistribution requires IEEE permission. See http://www.ieee.org/publications_standards/publications/rights/index.html for more information.

This article has been accepted for publication in a future issue of this journal, but has not been fully edited. Content may change prior to final publication. Citation information: DOI 10.1109/JSEN.2019.2907143, IEEE Sensors Journal

12. W. Qiu, X. Cheng, Y. Luo, Q. Zhang, and B. Zhu, "Simultaneous measurement of temperature and strain using a single Bragg grating in a few-mode polymer optical fiber", *Journal of Lightwave Technology*, vol. 31, no. 14, pp. 2419-2425, Jul. 2013.
13. M. M. Ali, S. F. Memon, E. Lewis, K. S. Lim and H. Ahmad, "Modal sensitivity enhancement of few-mode fiber Bragg gratings for refractive index measurement," 2016 International Conference for Students on Applied Engineering (ICSAE), Newcastle upon Tyne, 2016, pp. 308-311.
14. M. M. Ali, *Fabrication and characterization of few mode fiber Bragg gratings for mode conversion and sensing applications*, Ph.D. Thesis, University of Malaya, Kuala Lumpur, Malaysia, 2016.
15. H. Z. Yang, M. M. Ali, M. R. Islam, K.-S. Lim, D. S. Gunawardena, and H. Ahmad, "Cladless few mode fiber grating sensor for simultaneous refractive index and temperature measurement," *Sensors and Actuators A: Physical*, vol. 228, pp. 62–68, 2015.
16. O. Frazão, L. A. Ferreira, F. M. Araújo, and J. L. Santos, "Applications of Fiber Optic Grating Technology to Multi-Parameter Measurement," *Fiber and Integrated Optics*, vol. 24, no. 3-4, pp. 227–244, 2005.
17. Y. Zhao and Y. Liao, "Discrimination methods and demodulation techniques for fiber Bragg grating sensors," *Optics and Lasers in Engineering*, vol. 41, no. 1, pp. 1–18, 2004.
18. K. Lim, Z. Ong, Y. Lee, M. K. A. B. Zaini and H. Ahmad, "Pseudo high-Resolution Spectral Interrogation Scheme for Small Signals from FBG Sensors," in IEEE Transactions on Instrumentation and Measurement, vol. xx no. xx, pp. xxx-xxx, 2019. doi: 10.1109/TIM.2018.2871279.
19. A. Othonos, K. Kalli, Fiber Bragg Gratings: Fundamentals and Applications in Telecommunications and Sensing, Artech House, Norwood, 1999.
20. M. G. Xu, H. Geiger, and J. Dakin, "Modeling and performance analysis of a fiber Bragg grating interrogation system using an acousto-optic tunable filter," *Journal of Lightwave Technology*, vol. 14, no. 3, pp. 391–396, 1996.
21. J. Gong, J. Macalpine, C. Chan, W. Jin, M. Zhang, and Y. Liao, "A novel wavelength detection technique for fiber Bragg grating sensors," *IEEE Photonics Technology Letters*, vol. 14, no. 5, pp. 678–680, 2002.
22. J. Gong, C. Chan, W. Jin, J. Macalpine, M. Zhang, and Y. Liao, "Enhancement of wavelength detection accuracy in fiber Bragg grating sensors by using a spectrum correlation technique," *Optics Communications*, vol. 212, no. 1-3, pp. 29–33, 2002.
23. C. Chan, J. Gong, C. Shi, W. Jin, M. Zhang, L. Zhou, and M. Demokan, "Improving measurement accuracy of fiber Bragg grating sensor using digital matched filter," *Sensors and Actuators A: Physical*, vol. 104, no. 1, pp. 19–24, 2003.
24. G. Turin, "An introduction to matched filters," *IEEE Transactions on Information Theory*, vol. 6, no. 3, pp. 311–329, 1960.

Muhammad Khairol Annuar Bin Zaini received the B.Sc degree from the Department of Physics, Faculty of Science, Universiti Putra Malaysia, Malaysia, in 2015, and currently a postgraduate candidate at Photonics Research Centre, University of Malaya. His current research interest includes fiber Bragg grating sensors, and Spatial Division Multiplexing.

Yen-Sian Lee received the B.Sc. and M.Sc. in physics from the University of Malaya, Malaysia. He is currently pursuing his Ph.D. studies in the field of photonics engineering at Photonics Research Centre, University of Malaya, Malaysia. His current research interests include mode conversion technology for SDM system, fiber Bragg grating sensors and related technologies.

Kok-Sing Lim received the B.E. degree from the Department of Electrical Engineering, Faculty of Engineering, University of Malaya, Malaysia, in 2008, and the Ph.D. degree from the Photonics Research Centre, Department of Physics, University of Malaya, in 2012. He is currently a Senior Lecturer with the Photonics Research Centre, University of Malaya. He is a corporate member of Institute of Engineers Malaysia (IEM), a registered Professional Engineer (Telecommunication) with the Board of Engineers Malaysia (BEM) and a member of IEEE as well as OSA. His current research interests include fiber Bragg grating sensors, Spatial Division Multiplexing and laser medical devices.

Nurul Asha Mohd Nazal received the B.Sc. degree in Pure Physics from the School of Physics, University of Science Malaysia, in 2014 and the M.Sc. degree in Applied Physics from Department of Physics, Faculty of Science, University of Malaya, in 2016. She is currently pursuing the Ph.D. degree with the Photonics Research Centre, University of Malaya. Her research focuses on fabrication and characterization of regenerated gratings, thermal decay and analysis of regenerated gratings, thermal sustainability and related technologies.

Muhammad Mahmood Ali (GSM'14) received the B.S. degree in electronics engineering from the Islamia University of Bahawaplur in 2009, and the M.S. degree in electronics engineering from the Ghulam Ishaq Khan Institute of Engineering Sciences and Technology, Topi, Pakistan, in 2012. He is currently a Bright Sparks Ph.D. Fellow with the Photonics Research Centre, University of Malaya, Malaysia. His research interests include optical fiber sensors and lasers with applications, advanced digital signal and image processing, and microwave engineering. He is the member of the Pakistan Engineering Council and the National Academy of Young Scientists Pakistan.

1558-1748 (c) 2018 IEEE. Personal use is permitted, but republication/redistribution requires IEEE permission. See http://www.ieee.org/publications_standards/publications/rights/index.html for more information.

This article has been accepted for publication in a future issue of this journal, but has not been fully edited. Content may change prior to final publication. Citation information: DOI 10.1109/JSEN.2019.2907143, IEEE Sensors Journal

Harith Ahmad received the Ph.D. degree in laser technology from the University of Wales Swansea, U.K., in 1983. He is currently a Distinguished Professor with the Department of Physics, University of Malaya. He is the Director of the Photonics Research Centre with the University of Malaya, Kuala Lumpur, Malaysia. He is a Fellow of the Malaysian Academic of Science.

1558-1748 (c) 2018 IEEE. Personal use is permitted, but republication/redistribution requires IEEE permission. See http://www.ieee.org/publications_standards/publications/rights/index.html for more information.

This article has been accepted for publication in a future issue of this journal, but has not been fully edited. Content may change prior to final publication. Citation information: DOI 10.1109/JSEN.2019.2907143, IEEE Sensors Journal

1558-1748 (c) 2018 IEEE. Personal use is permitted, but republication/redistribution requires IEEE permission. See http://www.ieee.org/publications_standards/publications/rights/index.html for more information.

View publication stats